Lagrangian coherent structures and heat transport in compressible flows

Christian Lagares^{1,2} and Guillermo Araya^{2,a)}

¹Dept. of Mechanical Eng., University of Puerto Rico at Mayaguez, PR 00682, USA
²Computational Turbulence and Visualization Lab, Dept. of Mechanical Eng., University of Texas at San Antonio, TX 78249, USA

a)Corresponding author: araya@mailaps.org

Abstract. In this study, we delve into the intricate relation between Lagrangian Coherent Structures (LCS), primarily represented by the finite-time Lyapunov exponent (FTLE), and instantaneous temperature in turbulent wall-bounded flow scenarios. Turbulence, despite its chaotic facade, houses coherent structures vital to understanding the dynamical behavior of fluid flows. Recognizing this, we leverage high-fidelity Direct Numerical Simulation (DNS) to investigate compressible flows, focusing on the attracting manifolds in FTLE and their correlation with instantaneous temperature. The consequent insights into the coupling between fluid dynamics and thermodynamics reveal the profound influence of vortex stretching, shearing, and compression on local thermodynamic characteristics. Notably, the interplay of instantaneous static temperature and fluid properties, along with the cascading nature of energy in turbulent flows, underpins the observed correlation. Furthermore, we leveraged a high-performance, scalable volumetric particle advection scheme for LCS determination in subsonic ($M_{\infty} = 0.8$) and supersonic ($M_{\infty} = 1.6$) turbulent boundary layers over adiabatic flat plates.

INTRODUCTION

Turbulent fluid flows, despite appearing chaotic and random, often harbor coherent structures that underpin their dynamical behavior. The exploration and identification of these coherent structures (CS) are central to better understanding turbulence, since CS are responsible for most of the momentum and thermal transport phenomena. Among the various methodologies employed to decipher such structures, the concept of Lagrangian Coherent Structures (LCS) has emerged as a powerful and objective tool. Initially introduced by [1], LCS are identified through trajectories of mass-less particles, effectively organizing the flow into distinguishable regions. The backbone of LCS determination is the finite-time Lyapunov exponent (FTLE), shedding light on the rate of divergence or convergence of nearby trajectories in a flow field. High-speed turbulence, especially pertinent in aerospace contexts, requires meticulous study. High-fidelity numerical simulations, like Direct Numerical Simulation (DNS), offer detailed insights. DNS, a turbulence model-independent approach, may still be influenced by factors such as fluid type or molecular viscosity models in compressible flows. Once the rich data from DNS becomes accessible, it provides a fertile ground for extracting coherent structures. Notably, these structures can be studied either through an Eulerian or Lagrangian lens, each with its distinct advantages and implications. LCS, as a Lagrangian method, has been extended and adapted to various domains. From biological studies [2, 3], geophysical examinations [4], to ecological investigations [5], LCS's ubiquity underscores its significance. The inherent frame-independence and resolution insensitivity, as described by [1], render LCS a preferred method for many scientific applications. However, their full potential, particularly in the context of high-speed turbulence, remains to be tapped.

In this work, we embark on a novel exploration correlating attracting manifolds in FTLE with instantaneous static temperature in turbulent scenarios subject to subsonic and supersonic flow regimes. Leveraging two DNS studies over flat plates spanning incompressible to high-speed flow regimes [6, 7, 8], we aim to shed light on compressibility effects and Reynolds number impacts on LCS.

PARTICLE ADVECTION SCHEME AND FTLE/FSLE COMPUTATION

The Lagrangian Coherent Structures (LCS), or manifolds formed by particle trajectories in a fluid flow, can be approximated by finite-time Lyapunov exponent (FTLE) and finite-size Lyapunov exponent (FSLE) methods. Both measure

the deformation of a particle field differently. The FSLE assesses the time needed for a particle pair to achieve a particular distance, while FTLE integrates over a fixed period, irrespective of the distance between particles [9]. However, with proper calibration, both methods can yield similar results [10]. In this study, we leverage previous work to build a high-performance and scalable volumetric particle advection scheme applied to LCS [11]. The reader is referred to [11] for a more comprehensive overview of the particle advection methodology. The particle's trajectory, released at a specific time t_0 and location x_0 , is represented by the flow map and the velocity field. The FTLE is given by:

$$FTLE_{\tau}(\mathbf{x},t) = \frac{1}{|\tau|} \log \left(\sqrt{\lambda_{max}(C_{t_0}^t(\mathbf{x}))} \right), \tag{1}$$

where λ_{max} is the maximum eigenvalue and $C_{t_0}^t(\mathbf{x})$ is the right Cauchy-Green (CG) strain tensor at spatial coordinate \mathbf{x} . This tensor, defined as

$$C_{i,j} = \frac{\partial x_k^l}{\partial x_i^{l_0}} \frac{\partial x_k^l}{\partial x_j^{l_0}},\tag{2}$$

captures the deformation of a continuous body, describing the changes in material line length within the body due to deformation. Its eigenvalues represent the squared stretches along the principal material directions, while the eigenvectors denote the directions of these stretches. High FTLE values signify potential attracting or repelling manifolds. Forward time-integrated particle trajectories indicate repelling manifolds, whereas backward time-integrated trajectories denote attracting barriers [12].

DNS DATABASE

We are dealing with spatially-developing turbulent boundary layers (SDTBL) over adiabatic flat plates (or zeropressure gradient flow) and different flow regimes (subsonic and supersonic). Readers are referred to [6, 7, 8] for more details. The presently utilized DNS database were obtained via the inflow generation methodology proposed by [13]. The Dynamic Multiscale Approach (DMA) was recently extended to compressible SDTBL in [8] and [7] for DNS and LES approaches, respectively, which is a modified version of the rescaling-recycling technique by [14]. For both cases ($M_{\infty} = 0.8$ and 1.6), the friction Reynolds number (δ^+) range was approximately 700-900 with adiabatic wall thermal condition. The computational domain dimensions, in terms of the inlet boundary layer thickness δ_{inl} , were 15×3×3, along the streamwise, wall-normal and spanwise domain length, respectively. Mesh resolution in wall units: $\Delta x^+ \approx 11$, $\Delta y^+_{min} \approx 0.25$, $\Delta y^+_{max} \approx 11$, $\Delta z^+ \approx 10$. In both cases, the total number of grid points was 52M. The present DNS cases at high Reynolds numbers are run by using a highly accurate, very efficient, and highly scalable CFD solver called PHASTA. The flow solver PHASTA is an open-source, parallel, hierarchic (2nd to 5th order accurate), adaptive, stabilized (finite-element) transient analysis tool for the solution of compressible [15] or incompressible flows [16]. PHASTA has been extensively validated in a suite of DNS under different external conditions [17, 8, 7]. Figure 1 (left) shows the mean streamwise velocity by means of the van Driest transformation. Overall, a very good agreement can be observed with DNS by [18] at $M_{\infty} = 2$ from the near wall region up to the log region end. Small discrepancies are observed in the wake region that may be attributed to the different Mach number considered. Additionally, two different logarithmic laws have been inserted. A better fit of our predicted DNS values of U_{VD}^+ is observed with the logarithmic function $1/0.41ln(y^+) + 5$ as proposed by White [19] than the log law proposed by [20] (with a κ value of 0.38 and an integration constant, C, of 4.1). Moreover, a very good comparison is exhibited in fig. 1 (right) of present turbulence intensities and Reynolds shear stresses with DNS by [18], except in peaks of $u_{rms}^{\prime+}$.

MOST SIGNIFICANT RESULTS AND DISCUSSION

The Finite-Time Lyapunov Exponent (FTLE) serves as an invaluable diagnostic tool in discerning Lagrangian Coherent Structures (LCS) in complex fluid flows, and its interplay with instantaneous temperature in a compressible, turbulent boundary layer reveals a nuanced interaction between fluid mechanics and thermodynamics. At the forefront of this interrelation is the dynamic behavior of turbulence within the boundary layer. Such turbulence is characterized by vortex stretching, compression, and pronounced shearing, all of which considerably modulate local thermodynamic attributes. Consequentially, regions marked by high FTLE often mirror those of intense shearing and vortex stretching, where the mechanical work expended translates into discernible alterations in internal energy and, hence, temperature variations. This thermodynamic shift is not merely a passive response; it reciprocally influences the flow dynamics. Temperature fluctuations in compressible flows intrinsically modify fluid properties such as density and viscosity. As a result, zones exhibiting steep temperature gradients tend to also manifest amplified strain rates, further accentuating FTLE values. Moreover, the cascading nature of energy in turbulent flows, from larger to minuscule scales, culminates

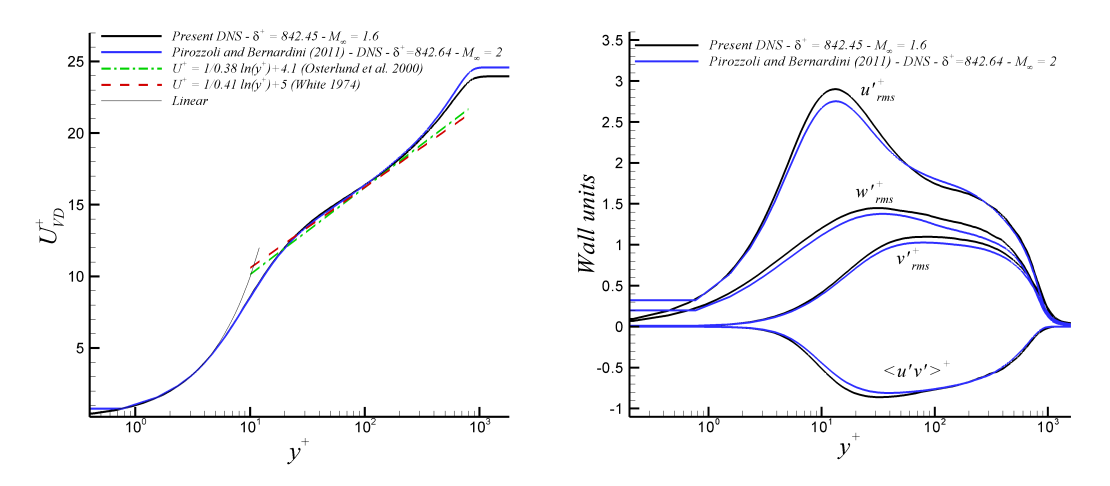


FIGURE 1: Van Driest transformation (left) and turbulence intensities and Reynolds shear stresses (right) in wall units for $M_{\infty} = 1.6$.

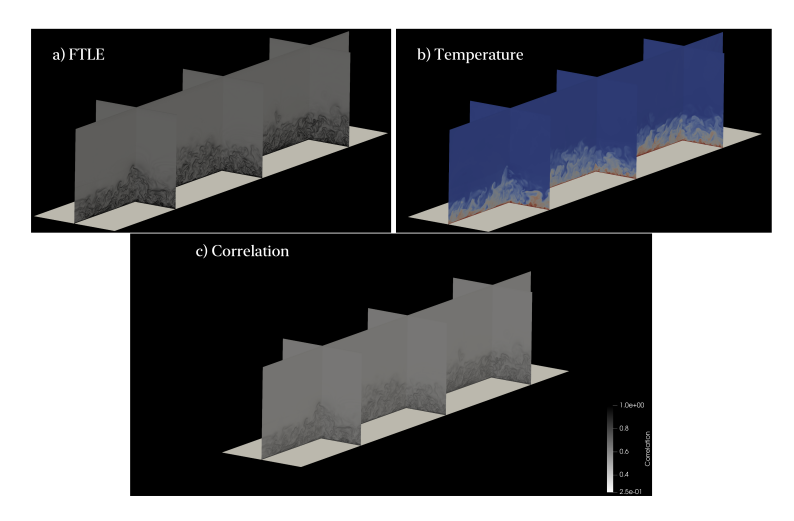


FIGURE 2: Contours of (a) FTLE, (b) static temperature, and (c) their cross-correlation at Mach 0.8

in kinetic energy dissipating as heat due to viscous actions, leading to localized temperature surges. This dissipation aligns with regions of heightened FTLE, indicative of the presence of smaller flow scales. Furthermore, the transport and advection mechanisms inherent in high FTLE regions can orchestrate the concurrent transportation of thermal structures. This intricate bond between momentum and heat transport, interwoven with the mechanical and thermodynamic changes within turbulent structures, offers a robust foundation for the observed correlation between FTLE and temperature in a compressible turbulent boundary layer. Figures 2 and 3 show the corresponding countours of attracting FTLE, instantaneous static temperature and their cross-correlation for the subsonic ($M_{\infty} = 0.8$) and supersonic case ($M_{\infty} = 1.6$). While the supersonic case depicts a higher level of isotropy in turbulent structures; the observed correlation between FTLE and static temperature is similarly high for both flow regimes: zones with large values of FTLE (high shear) indicate large concentration of temperature, and viceversa.

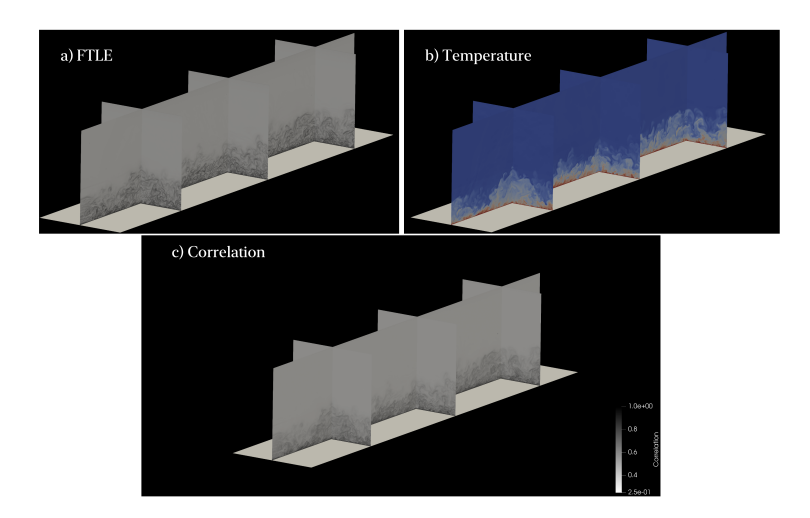


FIGURE 3: Contours of (a) FTLE, (b) static temperature, and (c) their cross-correlation at Mach 1.6

CONCLUSIONS

A significant similarity between FTLE (high shear zones) and static temperature concentration has been detected in subsonic and supersonic adiabatic flat plates via DNS. Future work implies the evaluation of lower Reynolds number cases to assess its influence as well as the computation of time-averaged FTLE-temperature cross-correlation profiles for better assessment of such quantities at different locations inside the boundary layer.

ACKNOWLEDGMENTS

This research was funded by the National Science Foundation under grants #2314303, #1847241, HRD-1906130, DGE-2240397. This material is based on research sponsored by the Air Force Office of Scientific Research (AFOSR) under agreement number FA9550-23-1-0241. This work was supported in part by a grant from the DoD High-Performance Computing Modernization Program (HPCMP).

REFERENCES

- [1] G. Haller and G. Yuan, Physica D **147**, 352–370 (2000).
- [2] J. Töger, M. Kanski, M. Carlsson, S. Kovacs, G. Söderlind, H. Arheden, and E. Heiberg, Annals of Biomedical Engineering 40 (2012).
- [3] S. Shadden, M. Astorino, and J. Gerbeau, Chaos **20** (2010).
- [4] F. J. Beron-Vera, M. Olascoaga, and G. Goni, Geophysical Research Letters 35 (2008).
- [5] J. Peng and J. Dabiri, Journal of Fluid Mechanics **623**, p. 75–84 (2009).
- [6] C. Lagares and G. Araya, AIAA SCITECH 2022 Forum (2022), 10.2514/6.2022-0479.
- [7] G. Araya and C. Lagares, Entropy **24** (2022), 10.3390/e24040555.
- [8] G. Araya, C. Lagares, and K. Jansen, 2020 AIAA SciTech Forum (AIAA 3247313) 6 10 January, Orlando, FL. (2020).
- [9] D. Karrasch and G. Haller, Chaos **23**, 1–11 (2013).
- [10] R. Peikert, A. Pobitzer, F. Sadlo, and B. Schindler, in *Topological Methods in Data Analysis and Visualization III* (Springer International Publishing Switzerland, 2014).
- [11] C. Lagares and G. Araya, Energies **16** (2023), 10.3390/en16124800.
- [12] G. Haller, Physica D: Nonlinear Phenomena **149**, 248–277 (2001).
- [13] G. Araya, L. Castillo, C. Meneveau, and K. Jansen, Journal of Fluid Mechanics 670, 518–605 (2011).
- T. Lund, X. Wu, and K. Squires, Journal of Computational Physics 140, 233–258 (1998).
- [15] C. H. Whiting, K. E. Jansen, and S. Dey, Comp. Meth. Appl. Mech. Engng. 192, 5167–5185 (2003).
- [16] K. E. Jansen, Comp. Meth. Appl. Mech. Engng. 174, 299–317 (1999).
- [17] C. Lagares and G. Araya, 2023 AIAA SciTech Forum (AIAA 3773400) 23 27 January, National Harbor, MD & Online (2023).
- [18] S. Pirozzoli and M. Bernardini, Journal of Fluid Mechanics **688**, 120–168 (2011).
- [19] F. M. White, Viscous Fluid Flow (McGraw-Hill Mechanical Engineering, New York, 2006).
- [20] J. M. Osterlund, A. V. Johansson, H. M. Nagib, and M. H. Hites, Physics of Fluids 12 (2001).